Proceedings of the 7th International Symposium on Cavitation
CAV2009
August 17-22, 2009, Ann Arbor, Michigan, USA

CAV2009 – 135

CAVITATION ANALYSIS OF A DOUBLE ACTING PODDED DRIVE DURING ICE MILLING

Roderick Sampson
Emerson Cavitation Tunnel
University of Newcastle, UK

Mehmet Atlar
Emerson Cavitation Tunnel
University of Newcastle, UK

Noriyuki Sasaki
National Maritime Research Institute
Japan

ABSTRACT

Propeller ice interaction is a complex phenomenon, which relies on innovative and complex experimental research in dedicated ice tank facilities. Whilst the ice tanks model the contact forces with good agreement, the hydrodynamic loading is often only assumed due to the inability to scale atmospheric pressure during these experiments. A small amount of research is however being conducted in cavitation tunnels using innovative methods to represent full scale ice milling conditions. Propulsor ice interaction tests in a cavitation tunnel are therefore both novel and uncommon due to their complexity. The Emerson Cavitation Tunnel at the University of Newcastle (ECT) has pioneered a series of ice milling tests within a cavitation tunnel using model ice. These ice milling tests allow an ice propulsor to experience correctly scaled cavitation numbers as a propeller interacts with ice. In all of the conditions tested, the current research observed presence and influence of cavitation and showed it to be a significant factor, something that is missing from standard ice tank tests. The work published in this paper forms part of a PhD research into the topic by the principal author [1].

INTRODUCTION

The design and construction of ice capable vessels is currently undergoing rapid expansion. At the forefront of this boom are the ice-capable double acting ships (DAS) outfitted with podded drives as reported by Sasaki et al. [2]. Since the launch of the double acting tanker, the DAS design has matured to include, container ships, tug boats and unconventional vessels like the *USCG Mackinaw* shown in Figure 1. The DAS concept is innovative; it allows vessels to advance stern first through level ice up to 1.5m thick at relatively even speeds of up to 3 knots. This continuous advance minimizes ice damage to the propulsor by avoiding the usual "*back and ram*" maneuvers that conventional shaft driven icebreakers must perform.

Figure 1: Double Acting ship *USCG Mackinaw* [3]

Despite the numerous benefits to this technology, the podded drives operate in a low-pressure wake of ice covered flows, which increases the likelihood of cavitation during ice blockage and ice milling. Under these circumstances the effect of cavitation during milling will be an essential factor for the performance and design of podded propulsors. To mitigate against these complex design conditions of low-pressure ice interaction, designers rely on physical model testing to make

informed design decisions. However ice research increases the complexity of contemporary hydrodynamic research and is often only resolved with costly and complex full-scale ice trials. Whilst ice tanks model a more representative ice cover scenario suitable for resistance and self-propulsion tests, they do not accurately scale the static pressure at the shaft line and this remains one of the numerous assumptions associated with model ice tank testing. Advances continue to be made, both in the mechanics of model ice and the ability to measure model scale ice loading more accurately. Despite numerous advances there is still relatively little published work into cavitation during model scale propeller ice interaction.

One of the first successful attempts at modeling cavitation during propeller ice interaction was Lindroos & Bjorkestam [4] who used a flat plate to simulate the ice clogging of a ducted propeller in a cavitation tunnel. The tests showed an increase in thrust and torque due to the blocked flow together with increased vibration and significant levels of cavitation. This paper showed for the first time that cavitation was an important aspect of propeller ice interaction, however the uptake of the findings was slow. Walker [5] expanded the work by Lindroos & Bjorkestam and studied the effect of ice blockage in a cavitation tunnel with a conventional R-Class propeller. Walker showed that whilst blockage elevated the thrust and torque loads for a propeller, the onset of cavitation in between ice block and propeller was quick to occur and had a significant impact on performance. Walker [5] showed that cavitation caused a reduction in the mean loads of thrust and torque but caused a significant increase in the dynamic time domain loads. The first ice milling tests at correctly scaled cavitation numbers were performed by Minchev et al. [6] who studied cavitation effects on an R-Class propeller in the Emerson Cavitation Tunnel (ECT). The work was successful and subsequently expanded by Atlar et al. [7] to study a DAS tanker propulsor. In both experiments the effect of cavitation was shown to be significant. Under cavitation numbers representative of full-scale ice milling conditions, both ice milling tests showed that the thrust load decreased upon ice impact where as the torque load increased on ice impact. The loss of thrust was attributed to the tremendous levels of cavitation present and the increase in torque was attributed to the mechanical ice contact load experienced by the propeller.

Recognizing the need for experimental ice milling data and to answer many unanswered questions from the earlier ice milling research, the milling tests at the Emerson Cavitation Tunnel were developed further into a broad, systematic PhD study into the phenomena [1]; this paper forms part of that study. The experiments were performed in 2 phases of ice blockage [8, 9] and ice milling [10, 11] shown in Figure 2. The research found that cavitation was a potential risk during propeller ice interaction, cavitation modified the propulsor performance, generated large levels of noise and vibration and posed a serious fatigue risk to the propeller and associated systems. Whilst useful ice research on podded propulsors continues in the ice tank community such as Wang [12], the effect of cavitation remains remiss.

Based on the above, the objective of this paper is give an understanding of cavitation during propeller ice interaction, to highlight it's effect on performance; to describe the types of cavitation present during propeller ice interaction and also to comment on it's erosive behavior on the propeller and ice blocks.

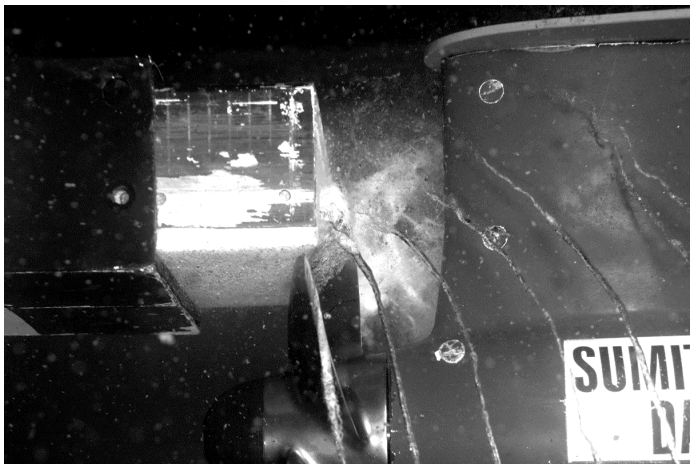

Figure 2: Cavitation extent as an ice block impacts a propeller

In this introductory section the objectives of the paper and its layout are given together with a short review of cavitation during propeller ice interaction. Following the introduction the experimental set-up is given. Next the results from the cavitation study are given including time series data of the interaction together with the observed cavitation. A description of the cavitation patterns is given together with the damage sustained by both the test blocks and the propeller during the experiment. The paper closes with a discussion on the influence of cavitation during propeller ice interaction and ask, "Does cavitation matter?" Finally conclusions and recommendations are made.

IMPLEMENTATION OF EXPERIMENT

The ice interaction tests were performed in the Emerson Cavitation Tunnel (ECT), which is a closed circuit depressurized tunnel located within the School of Marine Science and Technology at the University of Newcastle. The ECT has a measuring section of 3.2m x 1.2m x 0.8m and a contraction ratio of 4.274:1 with a maximum flow velocity of 8 m/s. Since the research in this paper was conducted the ECT has undergone a substantial upgrade to improve and automate the facility including the replacement of the measuring section and honeycomb. Figure 3 shows a schematic of the tunnel circuit and the basic specifications for the tunnel are given in Table I.

The propeller and pod body used in the experiment were a 1:31.2 scale model of a 16MW ice class azimuthing puller type podded drive fitted to the Sumitomo Heavy Industries (SHI) DAS tanker. The model propeller (P446) was manufactured from hydronalium PA20 and anodized red, whilst the pod body and fin were manufactured in hard plastic and painted to finish. Figure 4 shows propeller and pod housing used in the test while Table 2 displays the main particulars of the pod and propeller.

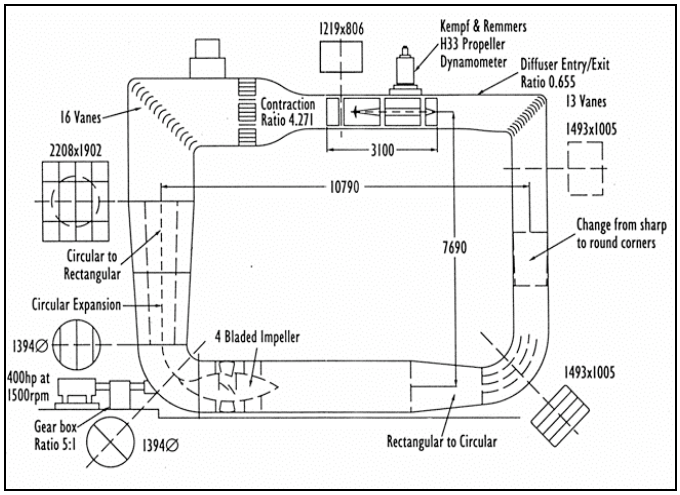

Figure 3: Emerson Cavitation Tunnel schematic.

Table 1: Emerson Cavitation Tunnel specification

Tunnel	Emerson Cavitation Tunnel
Facility type	Vertical, closed Circulating
Test section (LxBxH)	3.10m x 1.22m x 0.81m
Contraction ratio	4.271
Drive system	4 Bladed axial flow impeller
Main pump	300 kW
Impeller diameter	1.4 m
Maximum velocity	8 m/s (15.5 knots)
Abs. pressure range	7.6 kN/m2 to 106 kN/m2
Cavitation number	0.5 (min) to 23 (max)

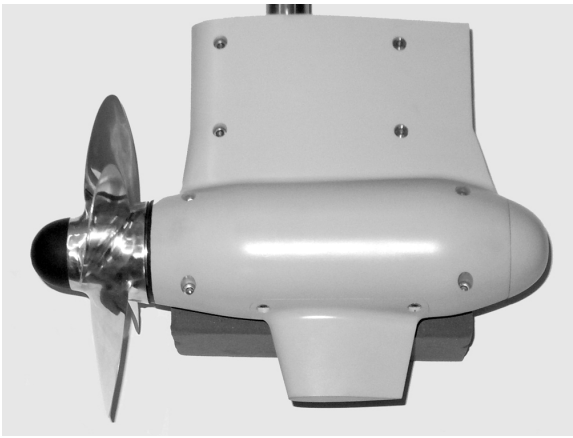

Figure 4: Photo of ice class podded propeller P446.

Table 2: Propeller P446 Characteristics

Scale	1:31.2	1:1
Number of blades	4	
Diameter	0.25mm	7.8m
P/D at r/R=0.7	0.692	
Blade area ratio	0.540	
Direction of rotation	Right	
Max. pod diameter	106.7mm	3.2m
Strut chord	220.7mm	6.62m
Strut span	131.7mm	3.95m
Max. strut thickness	51.3mm	1.54m

To perform blockage tests in the ECT a substantial test rig was needed to withstand tremendous suction forces whilst providing controllable delivery of the ice to the propeller race. Figure 5 shows a schematic of the test-rig set-up used in the cavitation tunnel tests; full details of the set-up are given in Sampson et al. [8]. Taking into account the restrictions imposed by the cavitation tunnel, it was not possible to use conventional model ice such as EG/AD/S, therefore a Styrofoam based material used in the previous milling tests in the ECT was again used. The foam (denoted S170 ice) was found to have a compressive strength of 170kPa, equivalent to first year ice, a sample is shown in Figure 6.

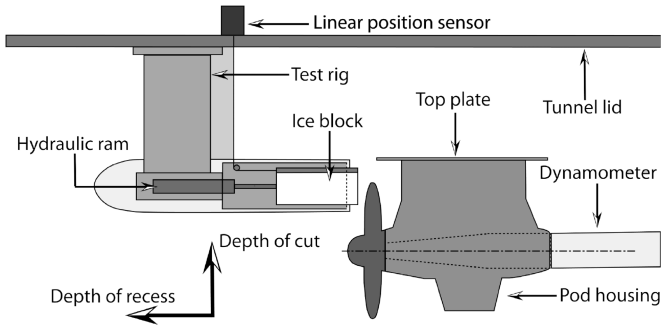

Figure 5: Blockage test rig setup in the ECT

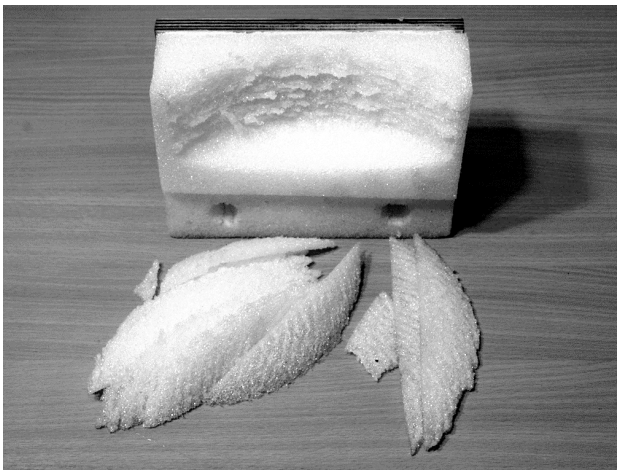

Figure 6: The complete test matrix of cast resin blocks

Table 3: Test parameters

Depth of cut (χ_c)	χ_c = 0.22, 0.33, 0.40
Feed rate (mm/s)	15
Tunnel velocity (m/s)	0.5 ~ 2.0
Cavitation Number (σ_n)	4, 3, 2, 1
Advance coefficient	0.26, 0.18, 0.12, 0.06
Milling stroke (mm)	56

The milling test consisted of a matrix of 80 blocks that were tested at 3 depth of cut (χ_c = ice depth / propeller radius) and a range of advance coefficients and cavitation numbers that were representative of full-scale milling conditions; the test parameters are given in Table 3. The air content was held between 25-35%; the model scale Reynolds number gave a

value typically ≥ $Re = 3.3 \times 10^5$ and the cavitation number based on the rotational velocity of the propeller was selected for practical convenience. Equation 1 gives the cavitation number; performance coefficients are given in Equations 2 – 3 and the Reynolds number is given in Equation 4.

Cavitation number $$\sigma_n = \frac{p - e}{\frac{1}{2}\rho(nD)^2} \quad (1)$$

Thrust coefficient $$K_T = \frac{T}{\rho n^2 D^4} \quad (2)$$

Torque coefficient $$K_Q = \frac{Q}{\rho n^2 D^5} \quad (3)$$

Reynolds number $$R_e = \frac{A_E / A_0}{Z} \times \frac{nD^2}{\nu} \quad (4)$$

EXPERIMENTAL RESULTS - DATA

Figures 7 ~ 9 show samples of the data for a typical milling scenario to provide an understanding of the typical load scenario during the interaction. Figure 7 shows the K_T and $10K_Q$ data for a propeller ice interaction event, the distance between ice block and propeller was reduced (left to right) from a blockage condition to full contact milling. The box shows the area of the interaction where the propeller contacted the ice and hence began ice milling. The smoothing function selected for the analysis was based on a *Loess* type filter as given by Cleveland & Devlin [13]. Inclusion of the raw time domain signals in the figure also highlighted the violent oscillatory nature of the test data especially during the milling period.

Figure 8 shows a $10K_Q$ backbone curve with key points identified to describe the different aspects of the interaction. At position (1) the ice block is moving towards the propeller, the propeller load at this point was due to the hydrodynamic open water load and the blockage effect created by the ice block wake. At point (2) the propeller experiences the maximum non-contact loading at axial distance (X_{px}), this position was known as the maximum proximity point. The difference in performance between point (2) and point (1) was due to the proximity of the ice block to the propeller. The proximity is effect has been explored extensively in the open literature by Shih & Zheng [14] and Bose [15] and is seen as a localized gain in K_T and $10K_Q$ due to partially obstructed flow. Beyond point (2) the leading edge of the propeller blade contacted the ice and the $10K_Q$ curve experienced a sharp drop (3) as it entered the impact zone (previously outlined with a box in Figure 7). The drop in $10K_Q$ during the impact zone was dependent upon operating condition and varied with depth of cut (χ_c). After the impact the $10K_Q$ curve recovered to a point above the maximum proximity point (4), this was due to the mechanical ice torque load. Finally the interaction settled into steady state milling at point (5). To clarify the different trends in performance due to cavitation Figure 9 shows K_T and $10K_Q$ against both time (s) and block position (X_B).

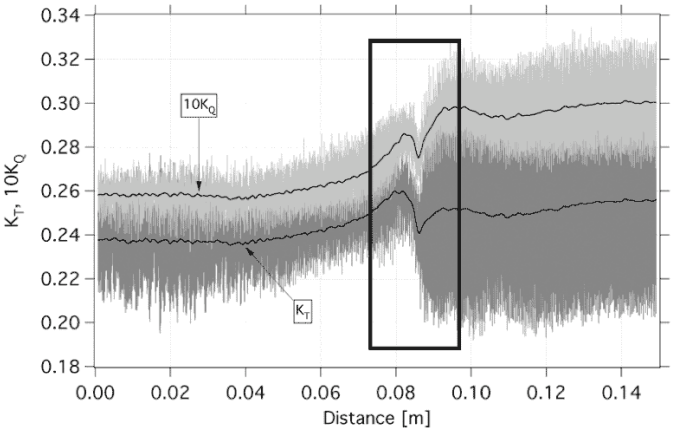

Figure 7: Ice milling time record showing the impact zone

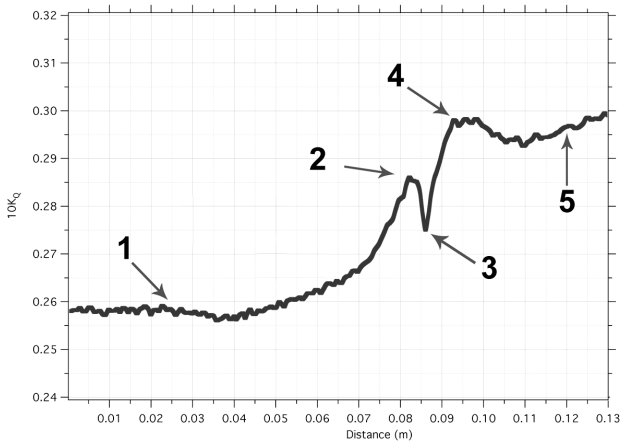

Figure 8: Ice milling phases recorded on the backbone curve

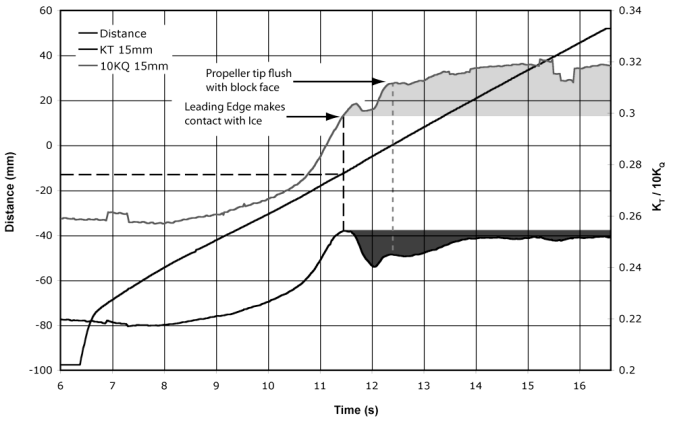

Figure 9: Change in K_T and $10K_Q$ during ice milling

Beyond the initial contact with the ice at *t = 11.5s* in Figure 9 the K_T curve fell below the maximum blockage load for the duration of the test, shown in dark grey. The loss in performance was due to the presence of severe cavitation and the disruption in lift over the blades caused by the milling process. The $10K_Q$ curve exhibited a very different trend and increased above the maximum blockage load for the full

duration of the milling test. This increase is shown in light grey on the figure and was consistent with an increase in $10K_Q$ due to the physical ice contact during milling.

The actual test data used in this paper is given in Figures 10 ~ 13 which show the K_T and $10K_Q$ test data measured at equivalent full scale 'double acting' mode conditions (J = 0.26). Two depths of cut are shown in the figures for $\chi_c = 0.22$ and $\chi_c = 0.40$ respectively. Due to space limitations the time domain torque curve was overlaid on the time domain thrust in the figures presented and therefore some overlap occurred of the time domain data. Additional comparative analysis of the backbone curves for each cavitation number tested in this set are also shown in Figures 14 ~ 15.

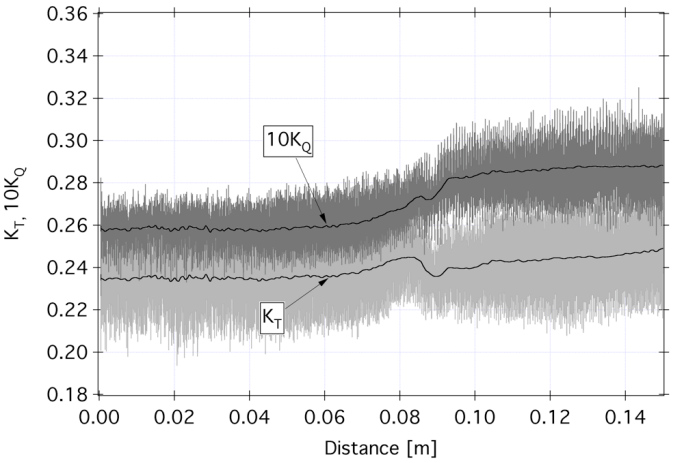

Figure 10: Propeller ice interaction $\chi_c = 0.22$, J= 0.26, $\sigma_n = 3.9$

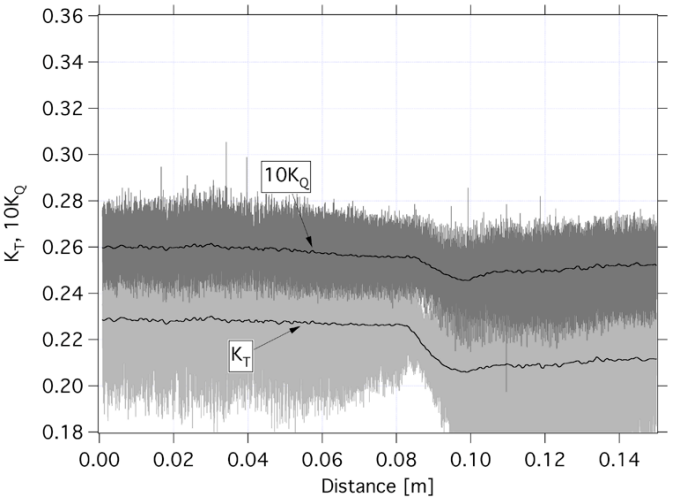

Figure 11: Propeller ice interaction at $\chi_c = 0.22$, J = 0.26, $\sigma_n = 1.3$

Figure 10 shows $\chi_c = 0.22$ at atmospheric conditions. This test showed the least sensitivity to the ice impact and milling process. In this figure impact occurred at approximately block position of X_B = 0.085m. Despite a small increase in performance due to proximity the smoothed blockage and milling loads were similar.

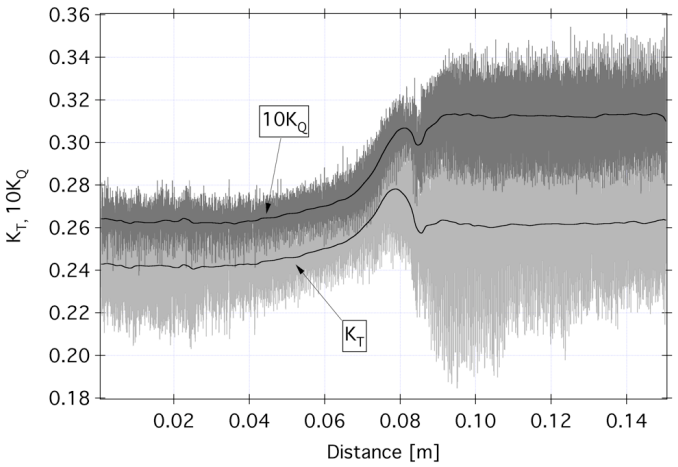

Figure 12: Propeller ice interaction $h_i = 0.40$, J= 0.26, $\sigma_n = 4.0$

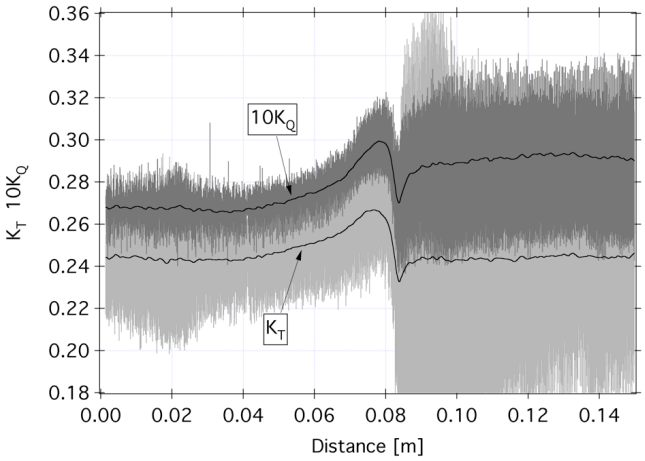

Figure 13: Propeller ice interaction at $\chi_c = 0.40$, J = 0.26, $\sigma_n = 1.4$

During milling the K_T in Figure 10 fell below the maximum blockage proximity value (X_{px}) whereas the $10K_Q$ showed a dip on ice impact and increased slightly above the X_{px} value. This was consistent with the findings of Figure 9. For the majority of conditions shown a dip (offload) was observed as the blades made first contact and impacted the ice blocks. The dip was generated from 2 possible scenarios, first an ice block pushes against the propeller during milling, effectively offloading the dynamometer shaft; this effect would be proportional to feed rate. A faster feed rate would cause the torque load to increase and the thrust to drop, however both terms dropped by similar amounts. The severity of the dip systematically changed with advance coefficient, reducing from $J = 0.26$ to $J = 0.0$. This supports the idea that the performance loss was a hydrodynamic effect. In Figure 11 the cavitation number was reduced to $\sigma_n = 1.3$. It is immediately evident in the figure that cavitation has increased the dynamic nature of the test data significantly. On contact with the ice (X_B = 0.085m), the cavitation was responsible for a significant drop in the backbone curves with both K_T and $10K_Q$ falling below the non contact condition.

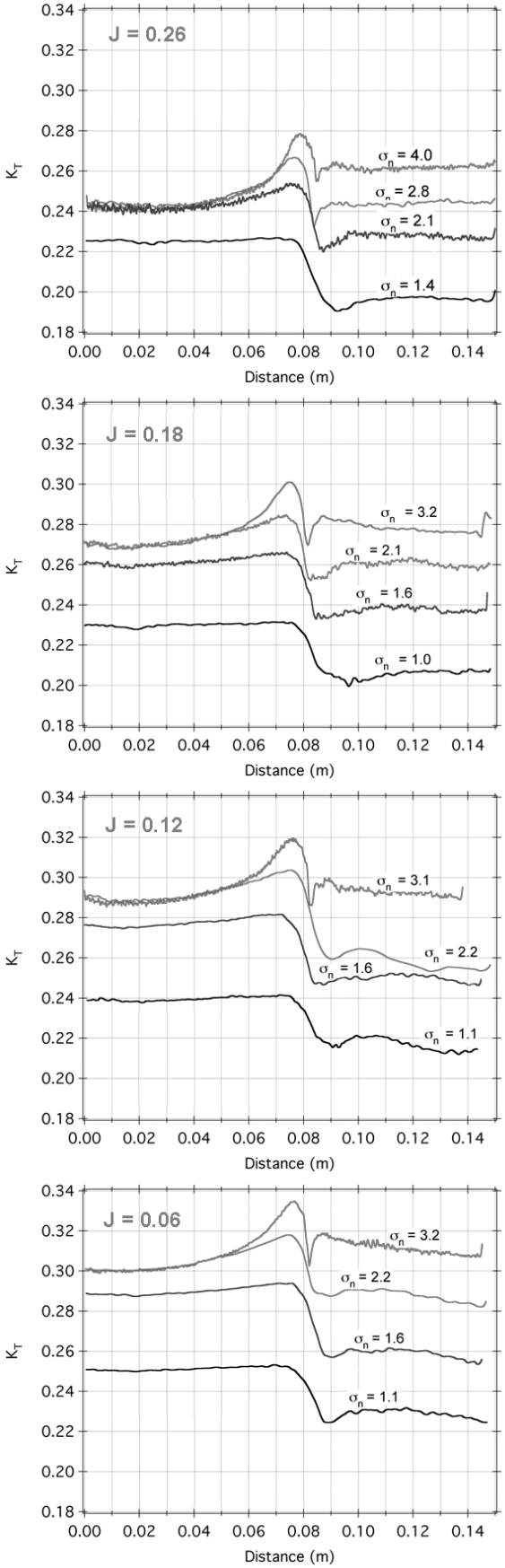

Figure 14: K_T Comparative analysis at $\chi_c = 0.40$

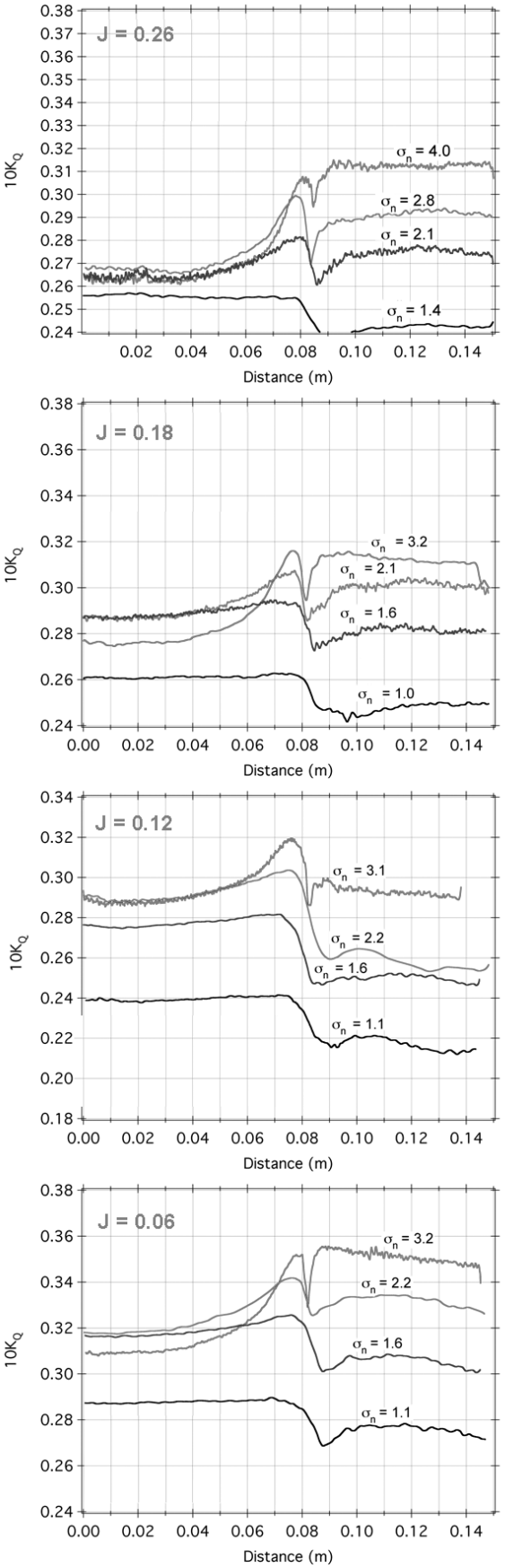

Figure 15: $10K_Q$ Comparative analysis at $\chi_c = 0.40$

Figures 10 ~ 11 illustrate very simply that whilst ice tank propeller tests can model some level of hydrodynamic propeller ice interaction, not scaling the cavitation number can have a significant effect on the measured propeller loads. The presence of cavitation therefore reduced the mean loads but significantly increased the dynamic loads. When the depth of cut was increased in Figures 12 ~ 13 for the same cavitation numbers, the effect although similar in nature, was larger in magnitude. In Figure 12 the proximity effect can clearly be seen to increase the K_T and $10K_Q$ backbone curves from the initial starting condition up to $X_B = 0.079$m when the propeller made contact with the ice. Therefore the K_T and $10K_Q$ backbone curves increased purely as a result of this larger depth of cut. Once the blades began to mill the ice there was the same performance dip and both K_T and $10K_Q$ experienced large loading oscillations due to the significant level of cavitation present. However when the cavitation number was reduced to $\sigma_n = 1.3$ in Figure 13, the volume of cavitation present in the ice cavity increased and the dynamic data for both K_T and $10K_Q$ became highly oscillatory. The additional cavitation developed in this condition prevented the K_T from recovering during milling and began to reduce any gain recorded for the $10K_Q$. Whilst the smoothed loading curve for both K_T and $10K_Q$ dropped as a result of the change in cavitation number, the cyclic loading recorded for the propeller increased dramatically. The non-contact proximity loading ($X_B = 0.00 \sim 0.079$) did not develop to a similar level as in Figure 12, however the performance drop as the blade made contact with the ice was more severe, this was indicative of the blade stalling or experiencing severe flow disruption. The impact point therefore represented the most violent and audible part of the ice interaction, the cavitation that had built up around the blades in close proximity to the ice became violent cloud and mist cavitation combined with ice debris around the podded drive; the effect stabilized during continuous milling but still remained extreme.

As the above mentioned figures represent a small part of the test program, Figures 14 ~ 15 were included to show the effect of cavitation on K_T and $10K_Q$ over a broader range of conditions as the advance coefficient was reduced to bollard pull mode. Whilst there was some scatter in the results it was clear that despite reduction in *J*, a reduction in the cavitation number caused a systematic reduction in the K_T and $10K_Q$ curves during milling. Not shown in the figures was the raw time domain data, which increased in amplitude dramatically. Therefore one of the main findings of the research was that the change in cavitation number was as significant on performance of an ice class propeller as the change in *J* for most of the milling cases observed.

EXPERIMENTAL RESULTS – CAVITATION IMAGES

Figures 18 ~ 19 show the cavitation photographs taken during the tests presented previously in Figures 10 ~ 13. The figures show the top part of the pod housing from the Port side during a milling event. In Figure 18 ($\chi_c = 0.22$, J = 0.26, $\sigma_n = 3.9$) the interaction was mostly a blockage phenomenon with a small level of ice penetration. For the portion of the blade in contact with the ice cloud and unsteady sheet cavitation was observed with a thin tip vortex present on all 4 blades.

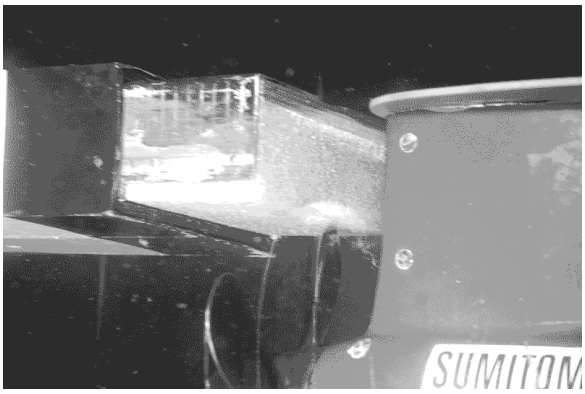

Figure 18: Cavitation at $\chi_c = 0.22$, J = 0.26, $\sigma_n = 3.9$

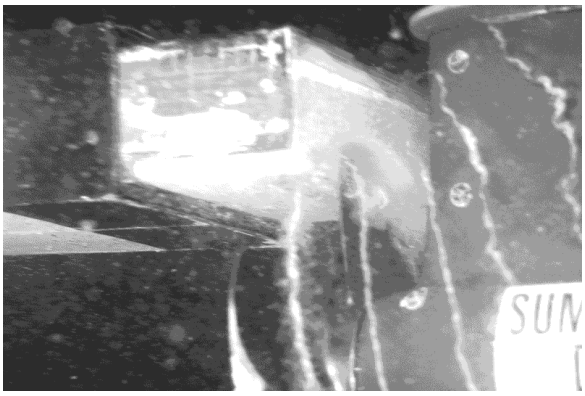

Figure 19: Cavitation at $\chi_c = 0.22$, J = 0.26, $\sigma_n = 1.3$

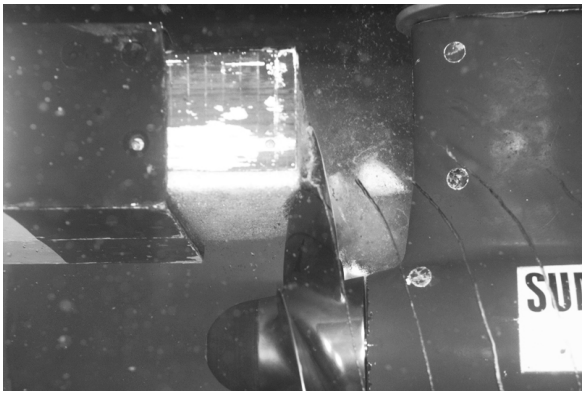

Figure 20: Cavitation at $\chi_c = 0.40$, J= 0.26, $\sigma_n = 4.0$

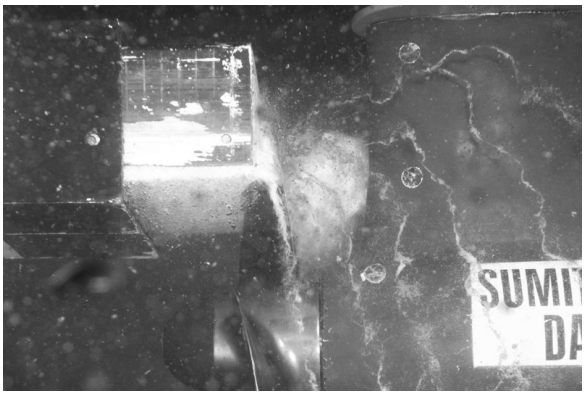

Figure 21: Cavitation at $\chi_c = 0.40$, J= 0.26, $\sigma_n = 1.4$

The reduction in cavitation number to $\sigma_n = 1.3$ in Figure 19 ($\chi_c = 0.22$, J = 0.26, $\sigma_n = 1.3$) caused dramatic increase in the level of cavitation, most noticeably the tip vortex has gained in size and become unsteady. In the ice cavity cavitation persisted as each blade passes through the recess with the most violent events of cavity collapse occurring at the exit of the blade from the block. For this experiment the collapse was responsible for significant levels of vibration and erosion of the test equipment and audible and often uncomfortable levels of noise.

When the depth of cut was increased to $\chi_c = 0.40$ in Figures 20 ~ 21 the cavitation present at both conditions was significant. In Figure 20 ($\chi_c = 0.40$, J= 0.26, $\sigma_n = 4.0$), the helix of the tip vortex was modified by the presence of the ice block as parts of the vortex filaments adjacent to the block were drawn toward it with the tip vortices bursting and impinging upon the strut of the pod. Any gap between the blade and the ice block was not only filled with violent cloud and mist cavitation, but combined with the debris and ice spall from the milled test block. Not seen on these images was the exhaust from the ice block, which was ejected on the starboard side. With a reduction in cavitation number to $\sigma_n = 1.3$ in Figure 21 ($\chi_c = 0.40$, J= 0.26, $\sigma_n = 1.4$), the tip vortex cavitation became more unstable and formed a volatile mixture of tip vortex cavitation, cloud cavitation and ice debris. It was common throughout the testing for the ice block and upper portion of the propeller to become completely obscured by cavitation.

EXPERIMENTAL RESULTS – CAVITATION PATTERNS

The video and still images recorded during the experiments were studied to obtain the cavitation pattern for $J = 0.26$ (double acting mode). Lower J values could have been selected however beyond $J = 0.26$ the structure of the cavitation such as tip vortex cavitation began to break down and was not always clear on the images. In addition the broad nature of the test restricted the analysis to the general trends in the cavitation behavior rather than specific examples. Figures 22 ~ 24 gives the changes in cavitation patterns due to ice milling. To simplify the presentation the most dramatic angular position ascertained from the video was examined, this was when the blade was close to the exit of the recess equivalent to 115° of rotation from the reference point entering the recess (directrix at 9 o'clock position). The lighter colored blade section in the figure denotes the reference blade and all cavitation patterns shown for this section relate to the back of the blade, any cavitation relating to the face of the blade was overlaid on the darker 3 remaining blades. A single tip vortex filament is also shown, this was truncated after 1 revolution for simplicity; the actual filament continued for several more revolutions but was not shown.

In tile (1) of Figure 22, the action of the propeller caused sheet cavitation to form on the block face due to the highly accelerated flow drawn from the underneath the blockage. The sheet cavitation between the blade and the block quickly broke down into unstable cloud cavitation as the blade continued to rotate. The low-pressure cavity caused the tip vortex filament to be drawn toward the block shown in tile (2) and not to leave the propeller tip along a helix of β_i as normal. Instead the tip vortex was bent towards the low pressure of the blockage wake shown as a flattening of the helix. With reduced proximity of the ice block the flow between the propeller and the ice block became more chaotic. In way of the stalled flow of the ice block and hence the higher pressure flow, the tip vortex cavitation violently burst between $\phi = 100° \sim 175°$ in tile (3). The proximity of the ice block here was the limit of the non-contact phase of the interaction, beyond this, impact and milling occurred.

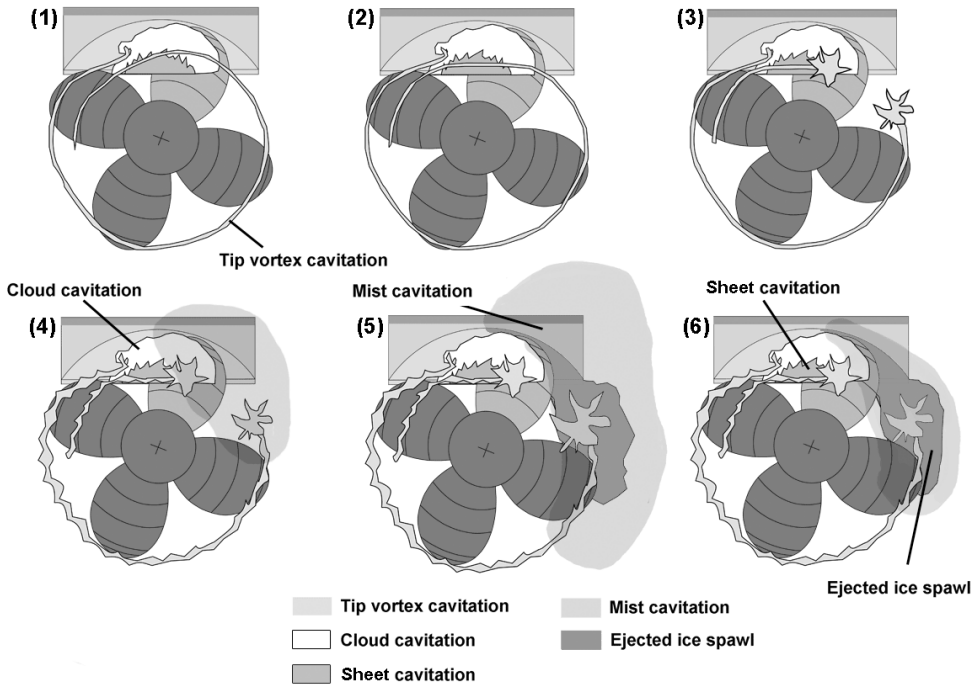

Figure 22: Ice milling cavitation patterns observed for $J = 0.26$ as the reference blade neared the exit of the ice block

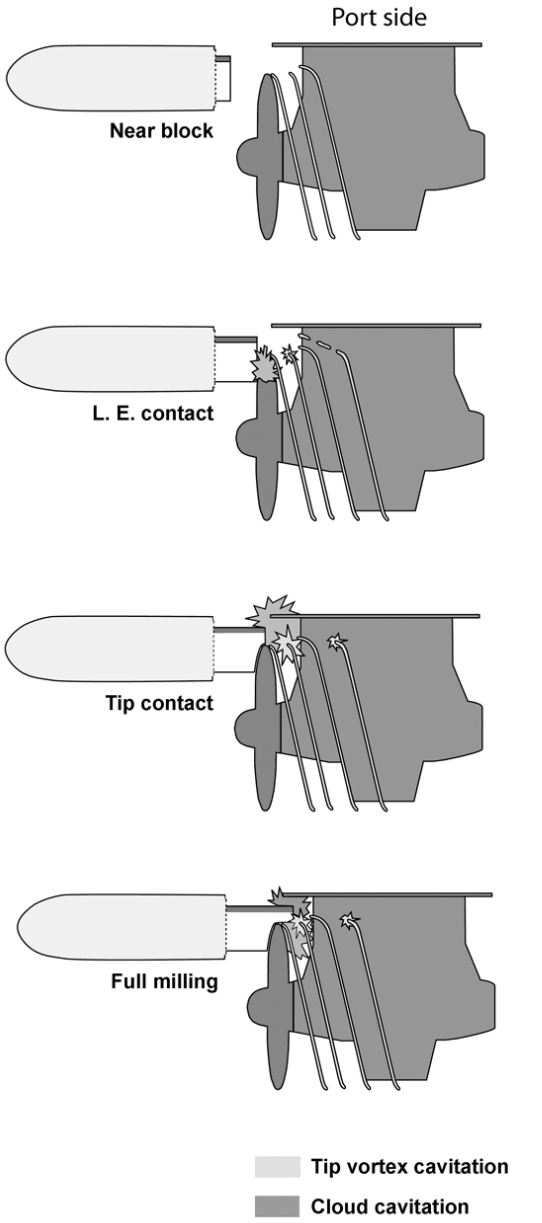

Figure 23: Port side cavitation patterns

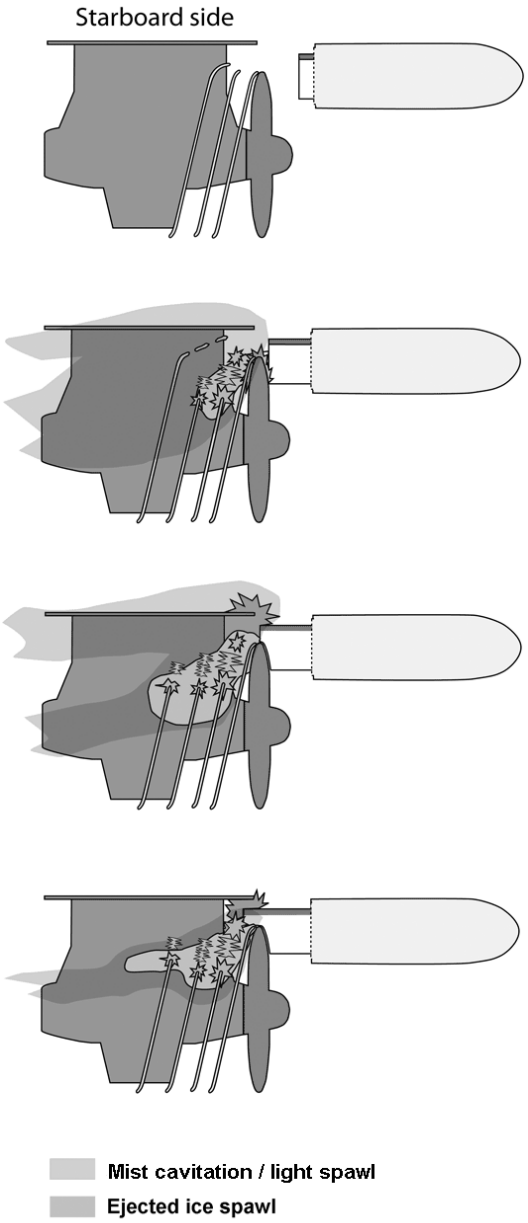

Figure 24: Starboard side cavitation patterns

Tile (4) shows the first stages of ice milling as the leading edge of the reference blade made contact with the ice; the tip vortex changed from stable vortex filament to unstable and often violent zones of unsteady cloud cavitation. The bursting phenomena observed in the latter part of the non-contact interaction gained intensity as the interaction proceeded. In addition to the cavitation, milled ice pieces began to be extruded from the damage zone. The transition of these pieces was influenced by the rotation of the propeller and the presence of the pod housing. Initially with a small amount of contact, the damage scattered like an explosion in all directions but focused quite clearly on the starboard side of the pod housing. The damage was typically a fine scatter of particles, which resembled a fine mist on the test video. As the interaction progressed in tile (5) the tip of the propeller made contact with the ice. The damage was scattered further upwards however at this point as the quantity of ice being removed increased and a clear cloud of particles could be seen crossing through the area of the bursting tip vortex cavitation and exhausted downstream. The tip vortex filament became full of ice particles and the reaction in general became very violent. The swept recess of the ice block by now was full of chaotic and violent cloud and mist cavitation as well as the ice spall being ejected. Finally in tile (6) the process reached steady state. In the previous tiles the impact process had sent ice pieces upwards and outwards on the exit side of the pod housing. In this instance the ice recess geometry played a significant part and focused the ejected ice pieces as they left the recess. Now the ice pieces were retained inside the fast moving jet stream of the propeller.

To further highlight the findings described above the lateral aspect of the cavitation patterns along the pod unit are shown in Figure 23 ~ 24 taken from the same analysis for a

representative J = 0.26 condition. The development of cavitation on the pod housing was asymmetric; therefore both sides of the housing are depicted. The Port side view was the most commonly photographed throughout the experiment; in this view the propeller was rotating towards the page and showed well defined cavitation patterns. The second view was the Starboard side of the pod and this lateral view provided diagnostic evidence on the cavitation and ice extrusion process. Therefore, 4 relevant conditions are shown for near block, leading edge impact, tip impact and full-contact milling conditions. However the development and path of the mist/spall extrusion was shown only for the starboard side case.

Figure 23 and Figure 24 showed that the near block condition did not generally exhibit significant changes to the cavitation patterns in excess of those observed in the open water condition. However, the reduced proximity caused a thickening of the vortex filaments and once close enough the development and thickening of sheet cavitation on the back of the blade in the ice recess. As with most pod propulsor testing, the vortex filaments were modified by the presence of the pod housing. The filament had a tendency to climb up the leading edge of the strut and then as it travelled along the chord of the strut the wake impinged on the strut wall. Once the ice interaction started however, the phenomena were quite different. The vortex filament was forced higher up the pod strut as the blade made contact with the ice. Just prior to the ice contact the tip vortex burst in way of the ice block exit, but most interestingly the top portion of the vortex filament in the path of the ice block was bent towards the ice blockage and flattened. The ice spall was only just being ejected at this point and it could be seen crossing the bursting tip vortex filaments causing them to expand into cloud/mist like haze and intensify. Coincident with this was the mist cavitation and ice spall that was thrown outwards and suffused as the interaction started. The debris was primarily focused on the starboard side but was thrown over the top of the pod housing, something not generally possible in ice tank testing. Once the propeller tip made contact with the ice block the damage pattern changed. There was an initial surge of ice spall and then the interaction quickly settled. The damage still suffused over the pod but there were now 2 branches to the damage path. The first over the top of the housing and the second following the joint of the nacelle and strut. The majority of the ice damage followed this later path, which was in line with the jet stream. Finally the milling became steady state as the ice cavity was milled and whilst the internal flow of the swept ice cavity became increasingly difficult to study, the external flow over the pod changed further. At this point the recess funneled the cavitation and ice debris into the slipstream of the propeller. The ice debris was no longer sprayed up and over the pod housing instead the geometry of the recess kept the damage to the nacelle/strut joint and within a narrow band of the slipstream; this interaction was observed on the majority of ice blocks tested.

Following completion of the ice milling test all of the test blocks were examined for cavitation damage a sample is shown in Figure 25. It is clear that significant levels of erosive cavitation were present, to damage the blocks particularly tiles (1) ~ (3). The damage was located on the block exit where the collapsing of the cloud cavitation combined with the bursting tip vortex occurred. Tile (3) represents a sample of advance coefficients and cavitation numbers. In general the most severe damage occurred with larger depth of cut and smaller cavitation numbers. The erosion patterns were measured on a single 20 second test, they represent a very short exposure time to the propeller.

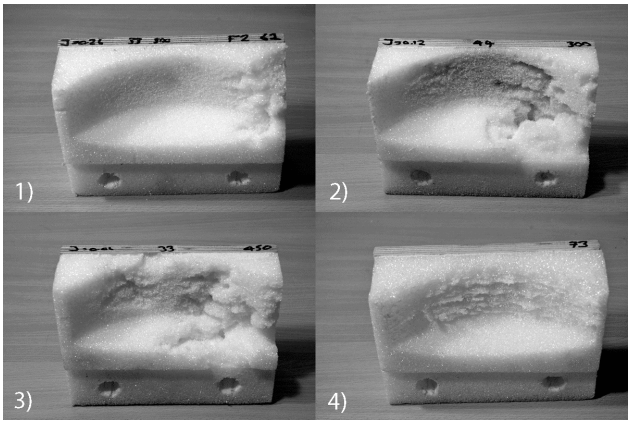

Figure 25: Cavitation damage to the test blocks

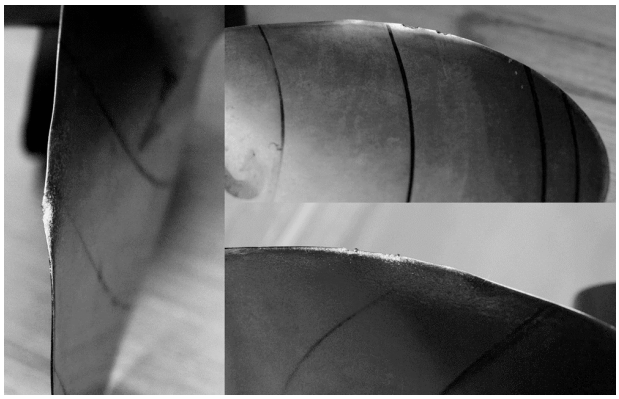

Figure 26: Cavitation damage to the model propeller

Finally Figure 26 shows the propeller used in the experiment, which suffered varying levels of erosive damage from exposure to cavitation. The blade location susceptible was the suction side trailing edge at r/R = 0.7 and the tests could have benefited from the use of a bronze propeller, however owing to weight restrictions this was not possible.

DISCUSSION

The objective of this paper was to advance the understanding and knowledge of propeller ice milling and in particular the effect of cavitation. During the course of the research, several papers were presented such as Sampson [8, 9], some received criticism for modeling an unrealistic or unnecessary scenario such as Naval Architect [16]. However, the research was a chance to ask `what if' questions about a phenomena, which as yet remains relatively un-researched under correctly scaled and systematic experimental conditions. The podded DAS drives have not had sufficient window of operation to consider them free from problems and contemporary ice tank tests rely on semi-empirical correction methods and experience to relate the results to full scale. As with conventional propeller testing in

ice tanks, the effect of cavitation cannot be modeled; the effect of cavitation during this process is therefore unknown. The findings in this paper have shown that propeller ice interaction contributes to a loss in mean performance but a dramatic increase in highly oscillatory blade loading due to cavitation, with obvious fatigue implications. Whilst the experiments were conducted with the support of Sumitomo Heavy Industries during construction of the first 2 double acting tankers *Tempera* and *Mastera*, they do not attempt to model a design condition, nor try to describe full scale operating conditions of these vessels explicitly; the test set-up would require modification to achieve this. The basis for the research was a systematic evaluation of ice interaction. In relating these findings to the 'double acting' design condition of the DAS tankers (J = 0.26 and σ_n = 4.1), the effect of cavitation would clearly be problematic.

There is also a trade off to be recognized with these vessels in so far as the ice class propeller by its very nature is stronger that a conventional propeller. Most designs are characterized by thick almost corpulent blade sections, smaller blade camber, less aggressive pitch distribution and benign blade outline shapes able to withstand ice impact. The effect of cavitation therefore may seem somewhat innocuous for these ice class designs. The model test plainly demonstrated the erosive nature of the interaction, the effect of cavitation not only manifest as erosive damage of the propulsor, as the test also showed the cavitation generated elevated levels of noise, something of concern in the eco-sensitive waters the DAS vessels sail through. Of greater concern to the operation of the vessels, apart from the loss of performance are the vibratory forces and the cyclic blade deflections, both in-plane and out-of-plane leading to the possibility of blade fatigue/failure. The current trend is for more of these DAS vessels to be introduced and these design questions need to be addressed.

The sea trials of the DAS tanker *Mastera* reported by Sasaki [2] under pinned the experimental design. Sasaki [2] reported ice ridge depths of 5 ~ 8m with ridge penetration even recorded up to 13.5m depth. On the actual trials of the DAS vessel *Norilsky Nikel* published by Wilkman et al. [17], the vessel (with a smaller draft than *Mastera* at 9m) was reported to operate in level ice of 0.5 ~ 1.5m at 2 ~ 3 knots. However on ice trials conducted between Murmansk to Yenisey River in March 2006, Wilkman et al. reported trials in ridges with ice thickness' of 5 ~ 10m. The vessel was able to penetrate these fields at a speed of 1 knot at 13MW, (full power) for 5 Nautical Miles, or 5 hours transit in restricted blocked/milling conditions. It is clear therefore that blocked and restricted flow conditions capable of reaching the propeller do exist and are not always transient. To assume that a propeller will not block or contact the ice during transit and should therefore not be studied in model scale contradicts all of the ice testing conducted thus far around the world. The assumption in ice tests is continuous ice contact to model a steady state phenomena, when in fact the loading is often transient. As ice tank testing is complex and still in its infancy when compared to more general performance testing in towing tanks and cavitation tunnels; more fundamental research is still required to tackle the problem.

At present only shaft torque is measured during full-scale trials; the main focus has been the ice torque loads. However given today's climate the inclusion of the system thrust would begin to understand the contribution of cavitation in the interaction. The thrust is typically obtained from hydrodynamic performance data from model tests, the thrust and torque curves respond differently in non-uniform flow and therefore may provide ambiguous results. This is particularly relevant as the use of the podded drive has changed the milling mode from an axial advance through the ice to a dynamic azimuthing of the pod at low speed. This new method allows the vessel to radially mill and flush the ice in an 'azi-milling' type motion and enables it to penetrate large ice ridges very quickly.

In terms of numerical modeling and prediction methods in ice, cavitation is marginalized in the calculations. This is not surprising as the variations in shaft and carriage speed in ice tanks result in a range of cavitation numbers for a single open water test such as Wang [12] with cavitation numbers ranging from σ_v = 5000 ~ 300 (σ_n = 130 ~ 30), in a similar manor the prediction tool developed do not consider cavitation either. For example Moores [18] suggested his design methods in the absence of cavitation, together with Newbury et al. [19] and Searle [20]. Whilst the desire for numerical models is simple linear trends, researchers are too quick to linearise a very complex system. The tests presented in this paper merely give a snapshot and suggest that the performance lost during ice interaction when compared to open water equivalents cannot simply be attributed to contact and milling loads. With this established, further work is required to harmonize work like Searle [19] and Wang [12] with the work presented here. In this approach a more accurate and rigorous model of propeller ice interaction can be achieved. This could then impose better design guidelines onto ice class propellers allowing the possibility of more structural optimization, reduced noise and increased efficiency.

CONCLUSIONS

This paper reports on a detailed set of cavitation experiments for a podded propeller during ice milling. Two conditions from the test program were studied for change in depth of cut, cavitation number and advance coefficient. Based on the analysis presented the following conclusions were drawn on the influence of cavitation in the interaction:

- Propeller ice interaction was highly dependent upon operating conditions and cavitation number.
- The change in cavitation number was as significant on performance of an ice class propeller as the change in J for most of the milling cases observed
- Cavitation contributes to a loss in mean levels of thrust and torque but causes and an increase in dynamic loading for propeller ice tests at low cavitation numbers.
- The cavitation during propeller ice interaction was shown to be significant. The blades experienced un-steady sheet and cloud cavitation as it milled the ice test block. The tip vortex was modified by the pres-

ence of cavitation and drawn towards the ice block, upon exit the tip vortex violently burst.

- As most numerical methods of predicting propeller performance in ice do not fully consider the effect of cavitation.
- The effect of cavitation is a relatively un-researched area of performance testing in ice. More work is required to address the many unanswered questions

REFERENCES

[1] Sampson (2009) "The effect of cavitation on propeller ice interaction" PhD, School of Marine Science and Technology, University of Newcastle [in submission]

[2] Sasaki, N., Laapio, J., Fagerstrom, B., Juurmaa, K., and Wilkman, G. (2004) Full scale performance of tankers Tempera and Mastera. Technical advances in podded propulsion (T-Pod), Newcastle upon Tyne, U.K.

[3] USCG Mackinaw, http://www.uscg.mil/d9/cgcMackinaw/, [Online source], accessed 20/5/2009

[4] Lindroos H. and Bjorkestam H. (1986) Hydrodynamic Loads Developed During Ice Clogging of a Propeller Nozzle and Means to Clear it. Polartech '86, Finland.

[5] Walker, D. (1997) The influence of Blockage and Cavitation on the Hydrodynamic Performance of Ice Class Propellers in Blocked Flow, PhD Thesis, Memorial University of Newfoundland.

[6] Minchev D., Bose, N., Veitch, B., Atlar, M. (1999) Propeller Ice Milling Tests in a Cavitation Tunnel. Report No. MT-1999-10 University of Newcastle, 1999

[7] Atlar, M., Prasetyawan, I., Aryawan, W. Sasaki, N. & Wang, D. (2003) Cavitation in Ice Milling Tests with a Model Podded Propulsor. 4th ASME JSME Joint Fluids Engineering Conference, Hawaii, USA

[8] Sampson, R., M. Atlar, and Sasaki, N. (2006) Ice blockage tests with a DAT tanker podded propulsor. Technical advances in podded propulsion (T-Pod 2006), Brest, France.

[9] Sampson, R., Atlar, M. & Sasaki, N. (2006). Propulsor ice interaction - does cavitation matter? Sixth international symposium on cavitation (CAV2006), Wageningen, The Netherlands.

[10] Sampson, R., M. Atlar, and Sasaki, N. (2007) "Effect of cavitation during systematic ice block tests", Port and Ocean Engineering under Arctic Conditions (POAC), Dalian, China.

[11] Sampson, R., M. Atlar, and Sasaki, N. (2009) Propeller Ice Interaction - Effect of milling, Port and Ocean Engineering under Arctic Conditions (POAC), Lulea, Sweden.

[12] Wang, J. (2007) "Prediction of propeller performance on a model podded propulsor in ice (propeller ice interaction)", PhD Thesis, Memorial University of Newfoundland, Canada.

[13] Cleveland, W. and Devlin, S. (1988) 'Locally weighted regression: An approach to regression analysis by local fitting", Journal of the American Statistical Association, Vol. 83

[14] Shih LY and Zheng Y. (1992) "Constricted Hydrodynamic Flow due to Proximate Ice Blockage over a Blade Profile in 2D". 2nd International Conference on Propellers and Cavitation, China.

[15] Bose, N., Veitch, B. & Doucet, M. (1998) "A design approach for ice-class propellers" Transactions - Society of Naval Architects and Marine Engineers Vol. 106.

[16] Uuskallio, A. (2008) "Milling tests contradicted" The Naval Architect, Royal institute of Naval Architects, London

[17] Wilkman, G. and Elo, M. and Lonneberg, L. and Kunnari, J (2007) "Ice Trials of MV Norilskiy Nikel in March 2006" Ports and Ocean under Arctic Conditions (POAC'07), Dalian, China.

[18] Moores, C. (2001) "Shaft and blade load measurements on highly skewed propeller model in ice" Masters of Engineering Thesis, Memorial University of Newfoundland, Canada.

[19] Newbury, S. and Browne, R.P. and Jones, S.J. (1994) "Experimental Determination of Hydrodynamic non Contact Loads during Propeller ice interaction", ISOPE '94, Vol. 2

[20] Searle. S. (1999) "Ice class Propeller Performance in Extreme Conditions", Transactions - Society of Naval Architects and Marine Engineers, Vol. 107.